



Master's Degree Thesis
ISRN: BTH-AMT-EX--2017/D17--SE

Design and Structural Analysis of a Jig-Fixture Assembly for a Tail Wing



**Burra Venkata Sai Vijay Krishna
Nallamothu Vamsi**

Department of Mechanical Engineering
Blekinge Institute of Technology
Karlskrona, Sweden

2017

Supervisors: Sankalp Guha, Tata Advance Systems, Hyderabad, India
Ansel Berghuvud, BTH

Design and Structural Analysis of a Jig-Fixture Assembly for a Tail Wing

Burra Venkata Sai Vijay Krishna

Nallamothu Vamsi

Department of Mechanical Engineering

Blekinge Institute of Technology

Karlskrona, Sweden

2017

Thesis submitted for completion of Master of Science in Mechanical Engineering with emphasis on Structural Mechanics at the Department of Mechanical Engineering, Blekinge Institute of Technology, Karlskrona, Sweden.

Abstract:

This thesis consists of two parts, the first part is about the structural analysis of a tail wing subjected to a face milling process to remove extra material from the tail wing. The focus of this part of the thesis is to check the stress distribution on the tail wing during the face milling process by simulating the CAD model of the tail wing by applying cutting forces which are estimated using Merchant circle diagram and evaluating its design strength by factor of safety which is found to be 2.1 suggesting the operation could be performed with given cutting parameters. The second part of the thesis is about the jig-fixture assembly designed for the milling operation on tail wing. This part of thesis precisely aims on verifying the design strength of the base plate of the assembly by estimating and applying the forces on the base plate during its transportation. Upon studying the stress distribution, the maximum stress was found to be 2.501 Mpa which when compared to yield strength of the material (205Mpa) is well within the limits suggesting the design strength to be acceptable for working loads.

Keywords:

4-Flute Cutter, Cutting Forces, Design Stability, Milling Operation, Merchant Circle Diagram.

Acknowledgements

This work is carried out at the Department of Mechanical Engineering, Blekinge Institute of Technology, Karlskrona, Sweden, under the supervision of Dr. Ansel Berghuvud.

The work is a part of a research project, which is a co-operation between the Department of Mechanical Engineering, Blekinge Institute of Technology and Tata Advance Systems, Hyderabad, India. This thesis work is initiated in February 2017.

We wish to express our sincere appreciation to Dr. Ansel Berghuvud for guidance and professional engagement throughout the work. At Tata Advance Systems, we wish to thank Mr. Sankalp Guha for valuable support and advice.

We wish to thank our parents for their constant support and love.

Karlskrona, October 2017

Burra Venkata Sai Vijay Krishna

Nallamothu Vamsi

Table of Contents

List of Figures	5
List of Tables	7
1 Notations	8
2 Introduction	10
2.1 Background	10
2.2 Problem Statement	11
2.3 Aim and Objectives	11
2.4 Research Questions	11
2.5 Related Course work	12
3 Method Overview	13
4 Literature Review	15
4.1 Milling Machines and Cutters	15
4.1.1 Column and Knee type	15
4.1.2 Manufacturing or Fixed bed type	16
4.1.3 Planer Type	16
4.2 Jigs and Fixtures	19
4.2.1 Jig	19
4.2.2 Fixture	20
4.3 Merchant Circle Diagram	25
5 Design Model	27
5.1 Truss	27
5.2 Top plate and the Peripherals	28
5.3 Base Plate	29
5.4 Final assembly	31
6 Finite Element Analysis	32
6.1 Structural Analysis of Tail Wing	32
6.1.1 Force Calculations	32
6.1.2 Simplifications	35
6.1.3 Analysis	35
6.1.4 Conclusion	35
6.2 Structural Analysis of Base Plate	35
6.2.1 Force calculations	35

6.2.2 Simplifications	37
6.2.3 Analysis	38
6.2.4 Result	41
6.2.5 Conclusion	42
7 Validation	44
7.1 Force Calculation	44
7.2 Simplifications	45
7.3 Analysis	45
7.4 Result	46
7.5 Conclusion	47
8 Design Iterations	49
8.1 Force Calculations	49
8.2 Analysis	50
8.2.1 Design Iteration - 1 (T = 35 mm)	50
8.2.2 Design Iteration - 2 (T = 30 mm)	50
8.2.3 Design Iteration - 3 (T = 25 mm)	51
8.3 Results	52
8.4 Discussions and Conclusions	56
9 Future work	59
10 References	60
11 Appendix	61
11.1 MATLAB CODE	61
11.2 Partitions	62
11.3 Results from FE – analysis	62

List of Figures

<i>Figure 2.1. Final assembly including tail wing</i>	10
<i>Figure 3.1. Method for Structural Analysis of base plate</i>	13
<i>Figure 4.1. Column and Knee Type Milling [3]</i>	15
<i>Figure 4.2. Bed Type Milling Machine [3]</i>	16
<i>Figure 4.3. Plano-Miller type Miller [3]</i>	16
<i>Figure 4.4. Up-Milling [3]</i>	18
<i>Figure 4.5. Down-Milling [3]</i>	19
<i>Figure 4.6. Template Jig [3]</i>	21
<i>Figure 4.7. Plate Jig [3]</i>	22
<i>Figure 4.8. Channel Jig [3]</i>	22
<i>Figure 4.9. Diameter Jig [3]</i>	23
<i>Figure 4.10. Leaf Jig [3]</i>	24
<i>Figure 4.11. Ring Jig [3]</i>	24
<i>Figure 4.12. Box Jig [3]</i>	25
<i>Figure 4.13. Merchant Circle Diagram [3].</i>	26
<i>Figure 5.1. Truss Structure.....</i>	27
<i>Figure 5.2. Truss Structure Drawing.....</i>	28
<i>Figure 5.3. Top Plate Design.....</i>	29
<i>Figure 5.4. Top Plate Drawing.....</i>	29
<i>Figure 5.5. Base Plate Design.....</i>	30
<i>Figure 5.6. Base Plate Drawing.....</i>	30
<i>Figure 5.7. Final Assembly Isometric View.....</i>	31
<i>Figure 5.8. Final Assembly Trimetric View.....</i>	31
<i>Figure 6.1. Cutting Force Calculation by Application.....</i>	34
<i>Figure 6.2. Force Diagram.....</i>	36
<i>Figure 6.3. Contact Set.....</i>	37
<i>Figure 6.4. Location of boundary conditions and loading</i>	39
<i>Figure 6.5. Convergence Plot.....</i>	40
<i>Figure 6.6. Von-Misses Stress Distribution on Baseplate</i>	41
<i>Figure 6.7. Deformation of Baseplate</i>	41
<i>Figure 6.8. Von-Misses Stress Distribution Baseplate Top view</i>	42
<i>Figure 6.9. Zoomed view of maximum stress on D-ring.....</i>	43
<i>Figure 7.1. Von-Misses Stress distribution on shell plate</i>	46
<i>Figure 7.2. Deformation of the 2D baseplate</i>	47
<i>Figure 7.3. Von-Misses Stress distribution 3D analysis.....</i>	47
<i>Figure 7.4. Von-Misses Stress distribution 2D plate.....</i>	48
<i>Figure 8.1. Von-Misses Stress distribution for 35mm thickness plate.....</i>	52

<i>Figure 8.2. Deformation of 35mm plate.....</i>	52
<i>Figure 8.3. Von-Misses Stress distribution on 30mm thickness plate</i>	53
<i>Figure 8.4. Deformation of 30mm plate.....</i>	53
<i>Figure 8.5. Von-Misses Stress distribution on 25mm plate</i>	54
<i>Figure 8.6. Deformation of 25mm plate.....</i>	54
<i>Figure 8.7. Variation of load on each D-ring with thickness</i>	55
<i>Figure 8.8. Variation of maximum stress with thickness</i>	56
<i>Figure 11.1. Partition on D-rings</i>	62
<i>Figure 11.2. Stress distribution with average element size 65</i>	62
<i>Figure 11.3. Stress distribution with average element size 60</i>	63
<i>Figure 11.4. Stress distribution with average element size 55</i>	63
<i>Figure 11.5. Stress distribution with average element size 50</i>	64
<i>Figure 11.6. Stress distribution with average element size 40</i>	64
<i>Figure 11.7. Detailed View of stress distribution on D-ring</i>	65
<i>Figure 11.8. Detailed view of Max Stress on Baseplate</i>	65

List of Tables

<i>Table 6.1. Cutting Parameters.....</i>	32
<i>Table 6.2. Comparison Between analytical and Application values</i>	34
<i>Table 6.3. Mass details</i>	36
<i>Table 6.4. Material Properties</i>	38
<i>Table 6.5. Maximum Stress V/s Yield Strength.....</i>	43
<i>Table 7.1. Actual Mass of the Components</i>	44
<i>Table 7.2. Maximum Stresses</i>	48
<i>Table 8.1. Thickness V/s Assembly Mass.....</i>	49
<i>Table 8.2. Maximum stress values.....</i>	55
<i>Table 8.3. Maximum Stress on 25mm baseplate.....</i>	57

1 Notations

A_d	Contact Area on D-ring
A_{2D}	Contact Area on D-ring of original geometry
C_v	Cutting velocity
D_c	Depth of cut
D	Diameter of milling tool
F	Force required to lift the assembly
F_2	Force required to lift the original design
F_3	Force required to lift Design iteration-1
F_4	Force required to lift Design iteration-2
F_5	Force required to lift Design iteration-3
F_{2D}	Force on D-ring of original geometry
F_r	Feed rate
F_s	Specific cutting force
F_t	Feed per tooth
k_{c1}	Specific cutting force for 1mm ² chip cross-section
L_A	Length of arc of contact
N	Spindle speed
N_i	Number of inserts
M	Mass of the assembly
P	Power required by the machine
P_d	Load on each D-ring in terms of Pressure
P_{2D}	Load on each original D-ring in terms of Pressure
P_{3d}	pressure on each D-ring for Iteration-1
P_{4d}	pressure on each D-ring for Iteration-2
P_{5d}	pressure on each D-ring for Iteration-3

P_c	Power required, from commercial application
p_z	Cutting force
p_{zc}	Cutting force from commercial application
p_{xy}	Resultant cutting force
r	Radius
T	Thickness of the Baseplate
T_d	Thickness of the D-ring
W_c	Width of cut
ε	Young's Modulus
σ_{max}	Maximum Stress
σ_{Yield}	Yield Strength
ρ	Density
ϑ	Poisson's Ratio
η_m	Efficiency of milling machine
θ	Angle traced by the radius

Abbreviations

FS	Factor of Safety
MCD	Merchant Circle Diagram
MCT	Mean Chip Thickness
MRR	Material Removal Rate
UTS	Ultimate Tensile Strength

2 Introduction

This thesis is carried out at Tata Advanced systems, where the primary work on defence aviation assembly is carried out. This chapter gives a brief introduction of the thesis work. For a clear and systematic approach, the entire thesis is divided into two parts, i.e. first being the structural analysis of the tail wing and second is the design and structural analysis of baseplate of the jig-fixture assemblage.

2.1 Background

A tail wing, ready for the assembly, is to be fixed to an Apache (fighter helicopter) at the industry. Due to design constraints, it is subjected for an after-machining process, i.e. face milling for chipping off the extra material from the final tail wing. Therefore, a suitable jig-fixture assembly is designed to carry out the machining process.

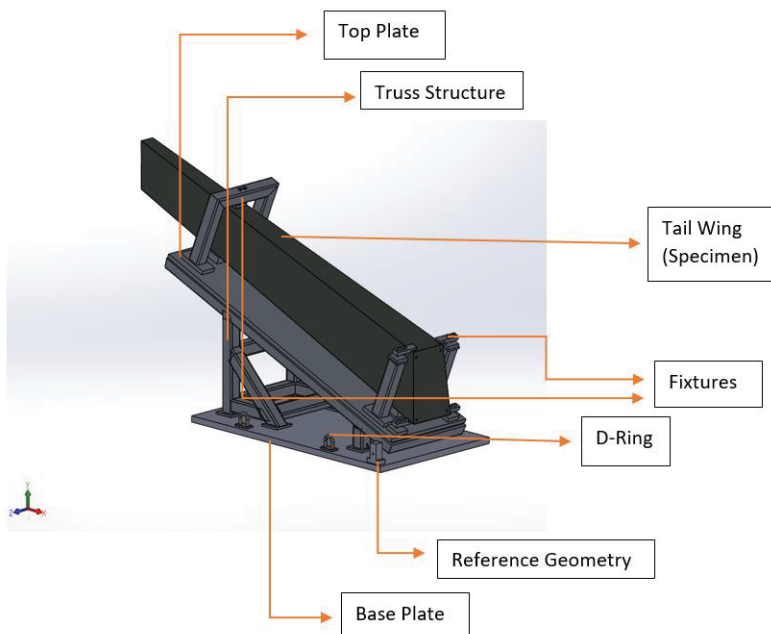


Figure 2.1. Final assembly including tail wing

2.2 Problem Statement

The first part of the thesis work is to check the design strength of the tail wing under the action of cutting forces during milling operation. As the milling process or the chipping off the material from the tail wing is close to the mounting points which are nothing but the holes or slots for fixing it to the Apache. Therefore, it is suggested to check the stress distribution around the mounting points.

The second part of the thesis work is to check the design strength of the baseplate of the jig-fixture assembly that is designed for lifting the entire assembly during its transportation.

2.3 Aim and Objectives

The aim of the first part of the thesis is to calculate the cutting forces from the milling tool on the work piece, i.e. the tail wing, import the CAD model of the tail wing into ABAQUS, study the stress distribution on the CAD model and evaluate the results by considering factor of safety as the criterion.

The aim of the second part of the thesis work is to estimate the loads acting on the baseplate when it is lifted off the ground, study the stress distribution on the CAD model of the baseplate and verify the design strength by comparing maximum stress on the plate with yield strength of the material.

2.4 Research Questions

1. Can the design sustain the milling operation with the given cutting parameters?
2. Can the baseplate sustain the weight of the entire structure when lifted during the transportation of the jig-fixture assembly without yielding?
3. What is the best possible thickness of the baseplate for the working loads that is readily available?

2.5 Related Course work

Some Literature on Merchant Circle Diagram and cutting tool profile is acquired from Metal Cutting Principle [1]. Literature on structural analysis of milling bed was found in a research paper [2]. This report gives an insight of force calculations from machine tools, checking the design strength. Also, provides design guide lines for future endeavours.

3 Method Overview

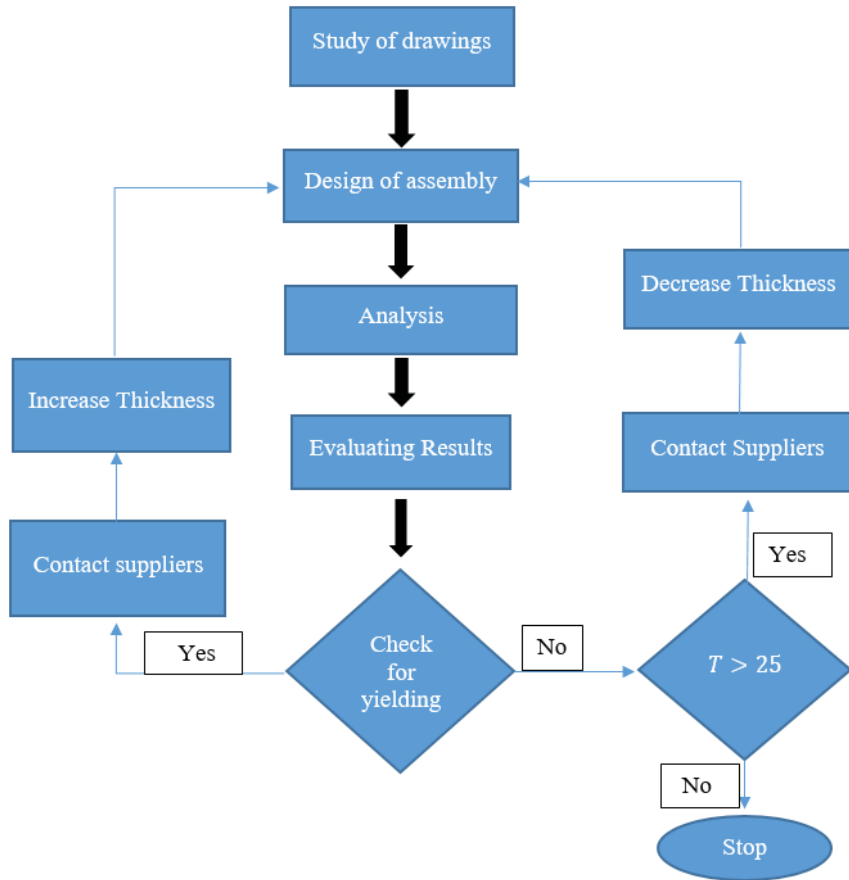


Figure 3.1. Method for Structural Analysis of base plate

The method of approach for Structural analysis of baseplate is depicted in the Figure 3.1. The method overview tree starts with study of drawings to make sure that the design is accurate with the actual design of Jig-Fixture assemblage.

On completion of design, the CAD model of the baseplate is imported to ABAQUS for analysis where the force calculations and the constraints are applied on the system.

Once the process is completed the design strength is evaluated by performing check for yielding, comparing the maximum Von-misses stress induced with the yield strength. If the design yields to the working loads, then suppliers of the raw material are contacted as various thickness are available with the them, upon increasing the thickness with same dimensions the problem of yielding could be resolved.

There are three different thicknesses in millimetres, readily available with the suppliers which are discussed under section Design Iterations. A Static analysis is performed on the all the designs available, would provide a good scope to the work and design guidelines.

4 Literature Review

4.1 Milling Machines and Cutters

Milling can be carried out in multiple methods. A milling machine is an equipment or a tool that helps chipping off the extra material from the work-piece that is fed in the opposite direction of the rotating cutter (single/multi flute cutter). The milling operators produce a better surface finish than the other conventional cutting procedures. Different types of millings are listed as follows:

4.1.1 Column and Knee type

A column and knee type milling is presented in the Figure 4.1. A Column and Knee type milling is used for both horizontal and vertical milling operations. The table holds the work piece against the spindle or the cutter rotation. The spindle/cutter rotates in a fixed position whereas the work piece is given a linear feed by adjusting or moving the table that is holding it. Different types of millings that fall under column and knee type are Hand milling, Plain milling, Universal milling, Vertical milling.

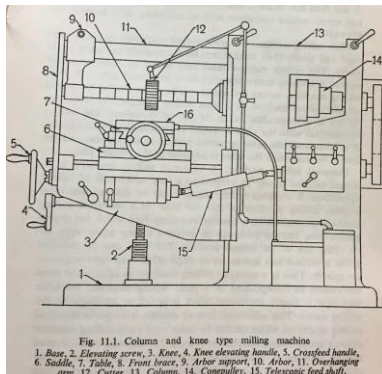


Figure 4.1. Column and Knee Type Milling [3]

4.1.2 Manufacturing or Fixed bed type

Figure 4.2 Shows a typical fixed bed type milling machine. In this milling type both the positions of work-piece and cutter can be altered simultaneously. The work piece is held by the table on the fixed bed which can only move in the longitudinal direction. The spindle or the cutter can only move in vertical direction. Fixed bed milling is categorised as Simplex milling, Duplex milling, Triplex milling.

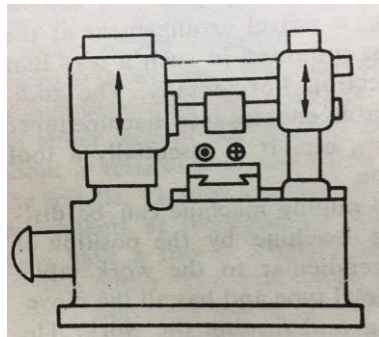


Figure 4.2. Bed Type Milling Machine [3]

4.1.3 Planer Type

Planer type is generally used to mill heavy work-pieces. The work-piece is clamped on the table which can only move in the Z- direction i.e., into the paper direction which is located on fixed bed. It consists of four cutters as shown in the Figure 4.3 that can move horizontally and vertically to perform milling operation.

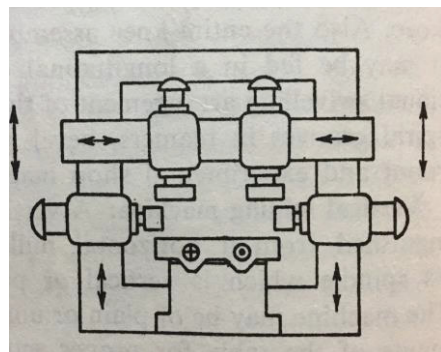


Figure 4.3. Plano-Miller type Miller [3]

Milling Machinery is mainly comprised of:

- 1) Base: It is the casting of grey cast iron which serves as the support or holding component for the entire milling machine.
- 2) Column: The column is mounted vertically on base that acts as supporting frame assembled with nuts and bolts that constraints unnecessary movements of the spindle and the table feed.
- 3) Knee: A Knee slides vertically of the column face. Screws mounted helps the component adjust the height. It also serves as house for feed mechanism of the table.
- 4) Saddle: The Saddle moves horizontally and its position can be altered by means of screw-nut arrangement to provide guideways for the table. It is located on top of the Knee and moves perpendicular to the column face.

Various processes performed by different milling cutters are grouped under three separate headings they are peripheral milling, face milling and end milling.

- 1) Peripheral Milling: This milling operation is carried out to produce the machine surface parallel to the axis of rotation of the cutter. For Peripheral milling, the cutting force is not constant throughout length of cut by each tooth due to which shock is developed in the driving mechanism that leads to vibration. Depending on the relative movement between the tool and the work, peripheral milling is furthered classified as.
 - a) Up Milling: Up milling is also known as conventional milling, wherein the cutter is rotated against to the work-piece travel. Figure 4.4 shows the working of Up milling. The chip thickness will be maximum when the cut terminates. The cutting force is directed upwards and this tends to lift the work-piece from the fixture. In this kind of a milling due to the typical nature of the cut, difficulty is experienced in pouring coolant just on the cutting edge from where the chips begin. As the cutter progresses, the chips accumulate at the cutting zone and may be carried over with the cutter spoiling the work surface. The surface generated by up milling appears to be wavy as the cutter teeth do not begin their cut as soon as they touch the surface. This process is the most widely used milling procedure even though it has so many disadvantages.

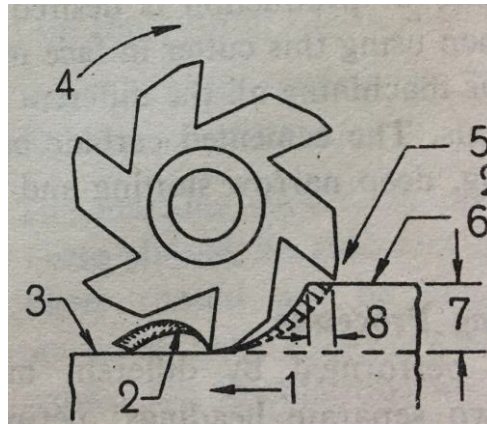


Figure 4.4. Up-Milling [3]

- b) Down Milling: Down Milling also called Climb Milling. In this process, the metal is removed by a cutter which is rotated in the same direction of travel of the workpiece. The working of down milling is shown in the Figure 4.5. Initially the chip thickness is maximum and reduces to minimum as the cut terminates. Unlike Up Milling, in Down Milling the cutter starts the cutting operation as soon as it touches the surface without slipping or sliding. In down milling, the position of the fixture becomes easy as the direction of the cut enables the fixture to sit and not get up in like up milling. The chips are also disposed easily, do not interfere with the cutting operation and the coolant can be poured directly over the cutting surface. The results obtained in down milling are much better than up milling the surface finish diminishes the heat generated. Even though down milling has so many advantages due to the backlash error in the old milling machines these are not used extensively.

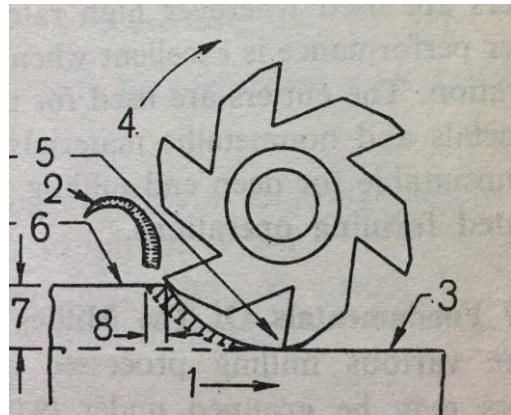


Figure 4.5. Down-Milling [3]

- 2) Face Milling: Face milling operations are performed to produce a flat machined surface perpendicular to the axis of rotation of the cutter. The peripheral edges of the cutter do the actual cutting, whereas the face cutting edges finish up the work by removal of very small amount of material. Both up and down milling may be performed, simultaneously on the work surface. The thickness of the chip is maximum at the end of the cut and minimum initially.
- 3) End Milling: End milling is a combination of both peripheral and face milling operation. The cutter has teeth on both the face and the periphery. The direction of helix of the cutter and the direction of rotation must be the same in end milling and vice-versa when peripheral cutting edges are being used.

4.2 Jigs and Fixtures

The jig and fixture are tool guiding and work-piece holding devices that are used during machining operation.

4.2.1 Jig

A Jig is defined as a device that holds and locates a workpiece, guides and controls one or more cutting tools. The holding of the work and guiding of the tool are such that they are in true positions relative to each other. In construction, a jig comprises of a plate, a structure, a box made of metal or in some cases non-metal having provisions for holding the components in identical positions one after the other, and then guiding the tool in correct

position on the work in accordance with the drawing, specification or operation lay out.

4.2.2 Fixture

A fixture may be defined as a device which hold and locates the workpiece during an inspection or for manufacturing operations. The fixture does not help in guiding the tool. In construction, a fixture comprises of a different standard or specially designed work holding devices, which are clamped on the machine table to hold the work in position.

The major advantages of using jigs and fixtures are listed below

- Eliminates the marking out, measuring, and other setting methods before machining.
- Increases the machining accuracy, because the workpiece is automatically located and the tool is guided without making any manual adjustment.
- Enables production of identical parts which are interchangeable. This facilitates the assembly operation.
- Increases the production capacity by enabling number of workpieces to be machined in a single set up, and in some cases handling time is also greatly reduced to quick setting and locating of work. The speed, depth of cut and feed for machining can be increased due to high clamping rigidity of jigs and fixtures.
- Reduces the operators labour and consequent fatigue as the handling operations are minimized.
- Enables semi-skilled operator to perform the operations as the setting operations of the tool and the work are mechanised. This saves labour cost.
- Reduces the expenditure on quality control of the finished products.
- Reduces the overall cost of machining by fully or partly automatizing the process.

The successful designing of a jig and fixture depends upon the analysis of several factors such as

- Study of the component

- Study of the type and capacity of the machine
- Study of loading and unloading arrangement
- Study of clamping arrangement
- Study of power devices for operating the clamping elements
- Study of clearance required between the jig and the component
- Study of the tool guiding and the cutter elements
- Study of the ejecting devices
- Study of rigidity and vibration problem
- Study of table fixing arrangement
- Study of methods of manufacture of the jig base, body or frame

The jigs and fixtures are classified into different types based on quality and complexity of the work or machining operation. Below mentioned are a few types of jig and fixtures [4].

- 1) Template Jig: It consists of a plate with two holes at required positions serves as template which is fixed on the component that is to be machined as shown in the Figure 4.6. The tool is guided through these templates and to carry out the machining process.

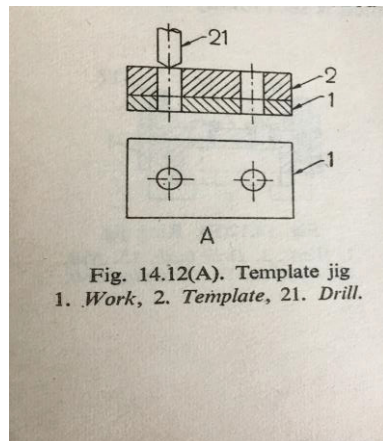


Figure 4.6. Template Jig [3]

- 2) Plate Jig: Figure 4.7 depicts a plate jig setup. Plate jigs are improvised versions of the template jig by incorporating drill bushes. The plate jigs are used to obtain higher accuracy and precision while machining.

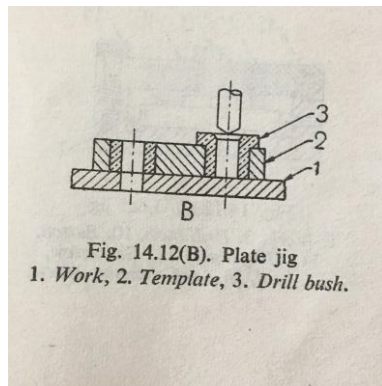


Fig. 14.12(B). Plate jig
1. Work, 2. Template, 3. Drill bush.

Figure 4.7. Plate Jig [3]

- 3) Channel Jig: A channel jig setup is presented in the Figure 4.8. A Channel jig consists of channel like cross section, where-in the work-piece is fixed by means of knurled knob.

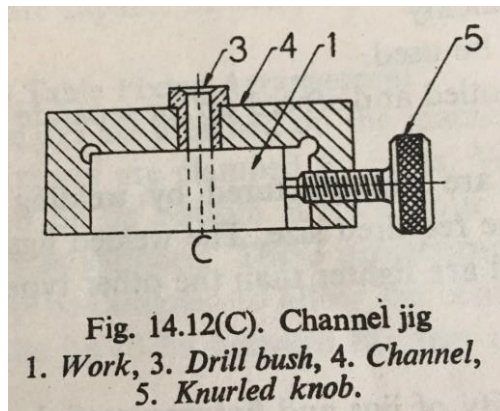


Fig. 14.12(C). Channel jig
1. Work, 3. Drill bush, 4. Channel,
5. Knurled knob.

Figure 4.8. Channel Jig [3]

- 4) Diameter jig: The Diameter jig is used in the cases where radial machining is involved. The work-piece is mounted on the V-Block and is clamped under clamping plate by means of clamping bolt as shown in Figure 4.9.

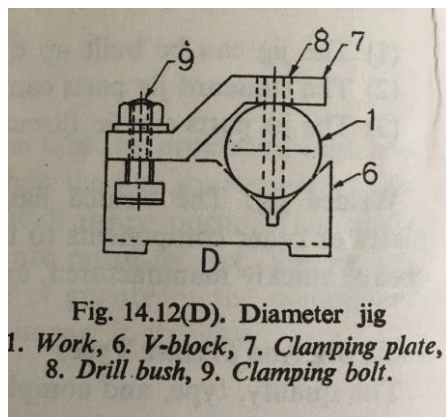


Fig. 14.12(D). Diameter jig
1. Work, 6. V-block, 7. Clamping plate,
8. Drill bush, 9. Clamping bolt.

Figure 4.9. Diameter Jig [3]

- 5) Leaf Jig: The Leaf Jig consists of hinge pin to open or close the jig, set screws and leaf clamping screws to constrain the motion of work-piece in horizontal and vertical direction as shown in the Figure 4.10. Due to complex mechanism, the work-piece might experience more clamping force compared to that of other Jigs.

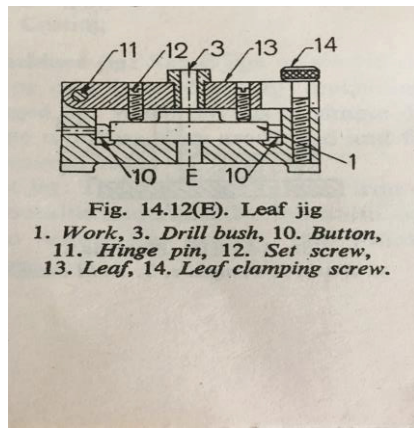


Fig. 14.12(E). Leaf jig

1. Work, 3. Drill bush, 10. Button,
11. Hinge pin, 12. Set screw,
13. Leaf, 14. Leaf clamping screw.

Figure 4.10. Leaf Jig [3]

- 6) Ring Jig: Figure 4.11 depicts the Ring jig setup. The Ring Jig is employed to machine circular flanged parts. The work-piece is clamped by means of clamping bolts is machined by the guiding the tool through the bushes.

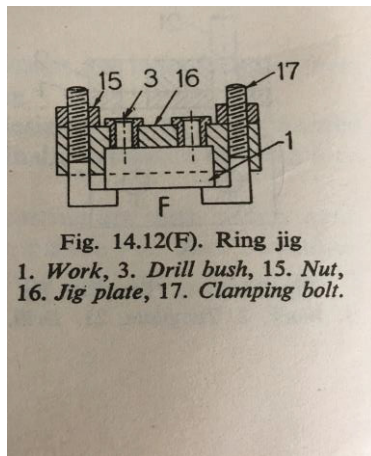


Fig. 14.12(F). Ring jig

1. Work, 3. Drill bush, 15. Nut,
16. Jig plate, 17. Clamping bolt.

Figure 4.11. Ring Jig [3]

- 7) Box Jig: A Box jig is used when there is a need for machining a work-piece at different angles and at different places. The main component is located by buttons within a box like construction. The cam clamps the work-piece and locates it as shown in Figure 4.12.

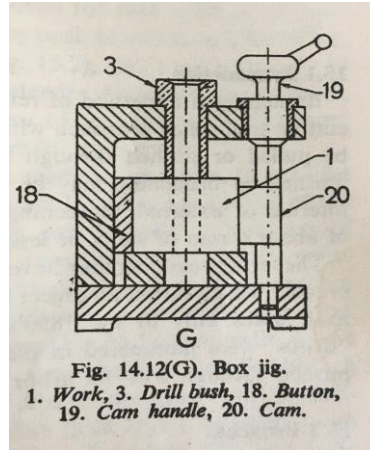


Fig. 14.12(G). Box jig.
1. Work, 3. Drill bush, 18. Button,
19. Cam handle, 20. Cam.

Figure 4.12. Box Jig [3]

4.3 Merchant Circle Diagram

- A Merchant Circle Construction [5] for Side face milling is proposed to study the cutting forces on the workpiece, i.e. Tail wing.
- A typical Merchant Circle Diagram is presented in the Figure 4.13.
- A reference line is constructed perpendicular to the cutting velocity.
- A suitable Scale is considered to convert Cutting velocity, C_v into Centimetres.
- Cutting force which is into the component, p_z is obtained by placing dynamometers on the component, p_z is scaled and marked on C_v . Also the perpendicular forces p_{xy} obtained from the dynamometer is scaled and extended perpendicular to C_v from the end of p_z
- The resultant of p_z and p_{xy} as diameter a circle is drawn which is Merchant circle, and the diagram is MCD.
- Rake surface is the surface of the work-piece with which the tool makes an angle.
- The Frictional force can be obtained by extending the Rake Surface to meet the Circle.

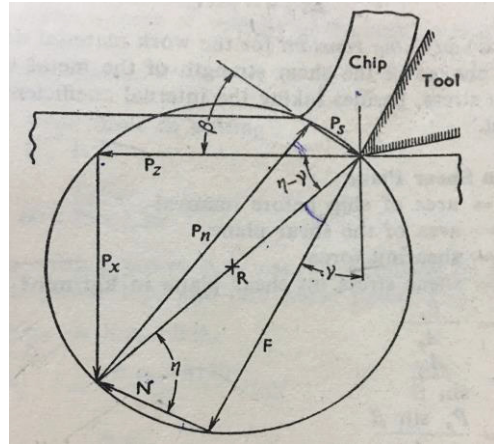


Figure 4.13. Merchant Circle Diagram [3].

From the MCD,

Feed Rate is the product of the spindle speed, number of inserts and feed per tooth.

$$F_r = N * N_i * F_t \quad (4.1)$$

Material removal rate is the product of depth of cut, width of cut and feed rate

$$MRR = D_c * W_c * F_r \quad (4.2)$$

Power, P required by the milling machine is given by the formula,

$$P = \frac{MRR * F_s}{\eta_m} \quad (4.3)$$

Also, P can be expressed as

$$P = p_z * F_r \quad (4.4)$$

Cutting force, p_z hence can be obtained.

5 Design Model

This section is related to the second part of the thesis work. The company denied sharing the design of the tail wing. The design procedure of Jig-Fixture is according to the design guidelines [6] and is as follows. The truss structure is designed initially followed by the top plate and the base plate at the end. The entire assembly is re-designed in Solid-works after the final check. The designs presented are re-designed as per the instructions and allowances provided by CAD engineers and supervisor at the Industry.

5.1 Truss

The truss structure is designed in such a way that it supports the top plate which is holding the work-piece, i.e. the tail wing of the Apache. The truss is inclined at an angle 22.49° with vertical to make the Tail wing's face perpendicular to the ground for face milling. Figure 5.1 and Figure 5.2 show the design and dimensions of the Structure in inches scaled 1:10 respectively.

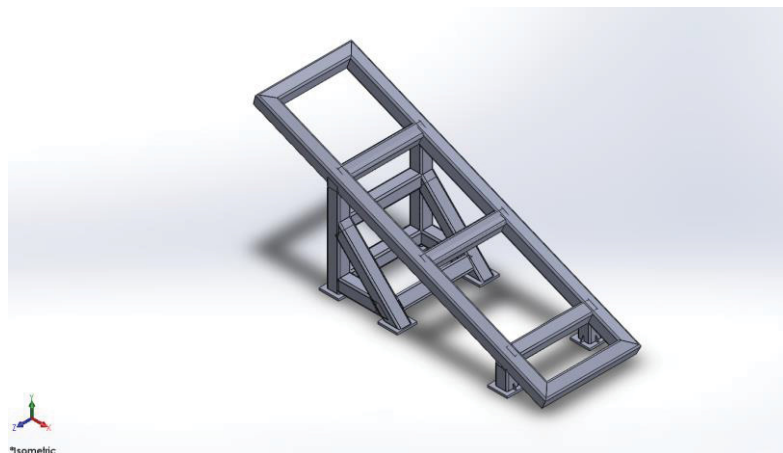


Figure 5.1. Truss Structure

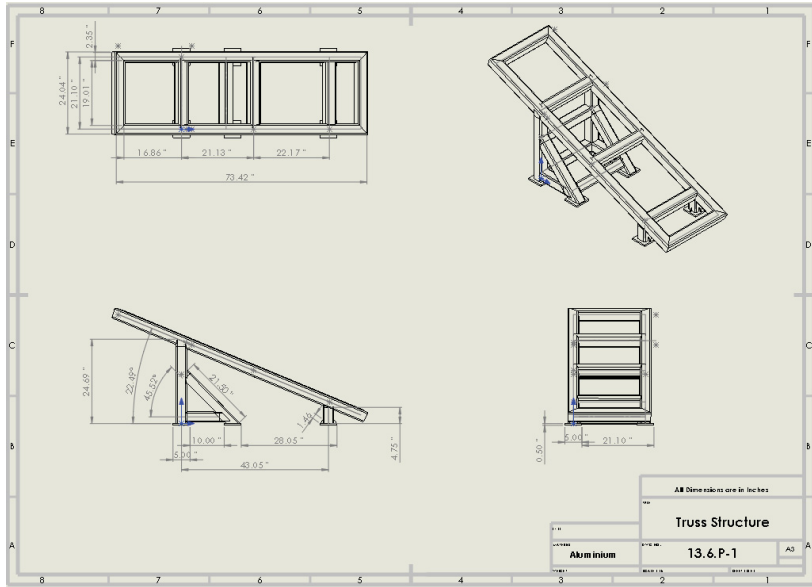


Figure 5.2. Truss Structure Drawing

5.2 Top plate and the Peripherals

Figure 5.3 shows the design of the Top plate of the assembly. Top plate and the peripherals play a vital role in this jig and fixture arrangement as they hold the workpiece firmly. The workpiece rests on the top plate and the peripherals consists of butts, bridge clamps [6] and an anchor that holds the workpiece from the top. The peripherals and the holders are completely adjustable by screw-nut mechanism. The top plate is fixed on to the truss structure. Butts are placed to hold the workpiece in position so that the milling operations takes place through the guided region. Figure 5.4 gives a clear information of the dimensions of the top plate as well as the peripherals along with their positions.

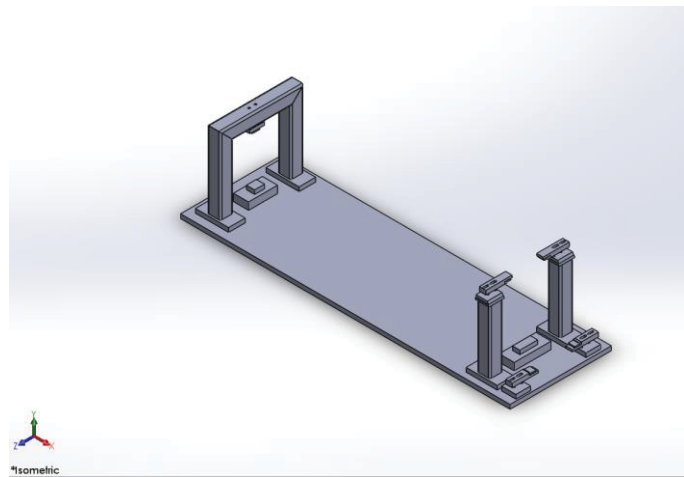


Figure 5.3. Top Plate Design.

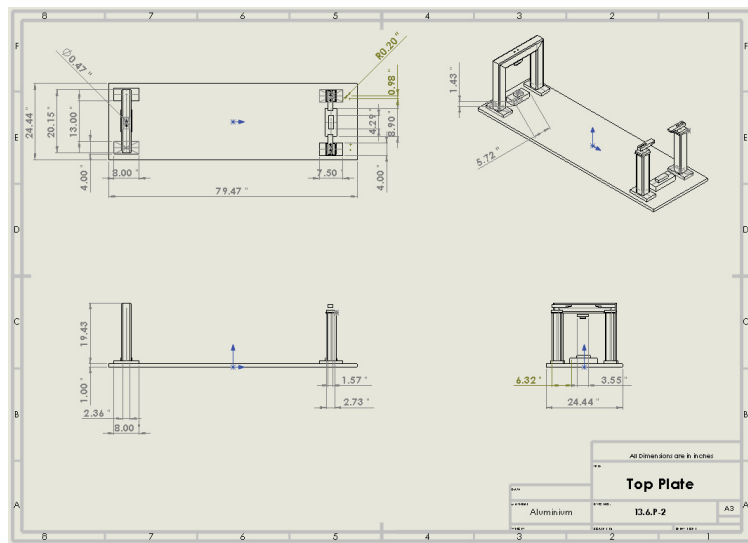


Figure 5.4. Top Plate Drawing.

5.3 Base Plate

The design of the baseplate is shown in the Figure 5.5. This base plate is the support structure that rests on the ground and bares all the weight. The base plate plays a very vital role in providing strength to the structure. The truss

structure along with the top plate rests on the baseplate. The base plate also comes with four d-rings which allow to fix hooks that help in the transportation of the jig and the fixture. The base plate is made of Aluminium-5052. The drawings shown in the Figure 5.6 are presented to the manufacturing engineers.

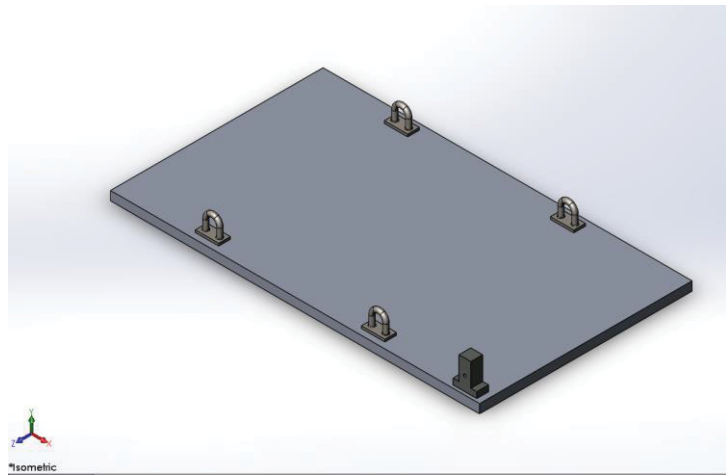


Figure 5.5. Base Plate Design.

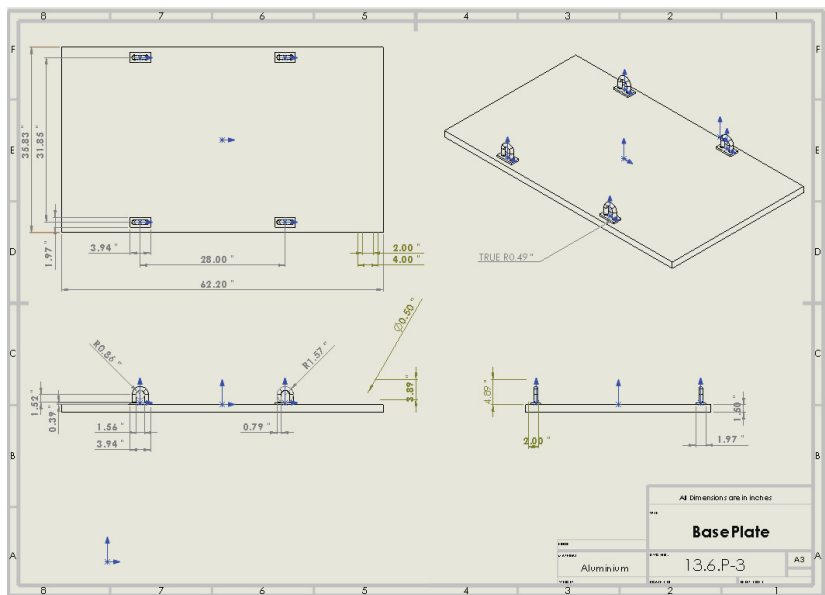


Figure 5.6. Base Plate Drawing.

5.4 Final assembly

The Truss structure, base plate, top plate and the tail wing are assembled as per the design specifications from the industry. The Tail wing in Figure 5.7 and Figure 5.8 is a specimen but not the actual design of the tail wing.

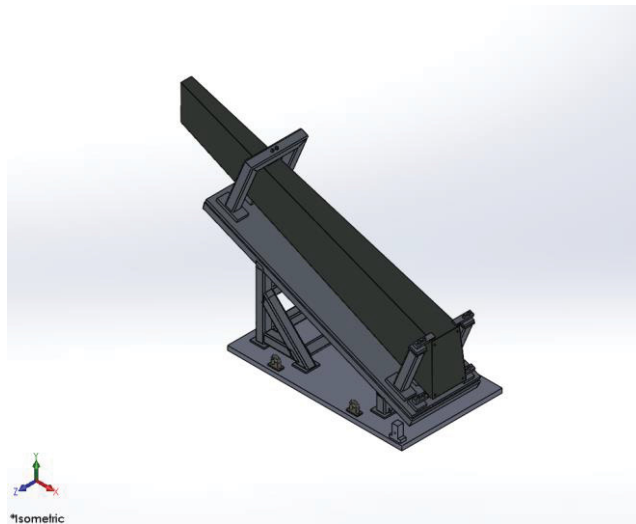


Figure 5.7. Final Assembly Isometric View

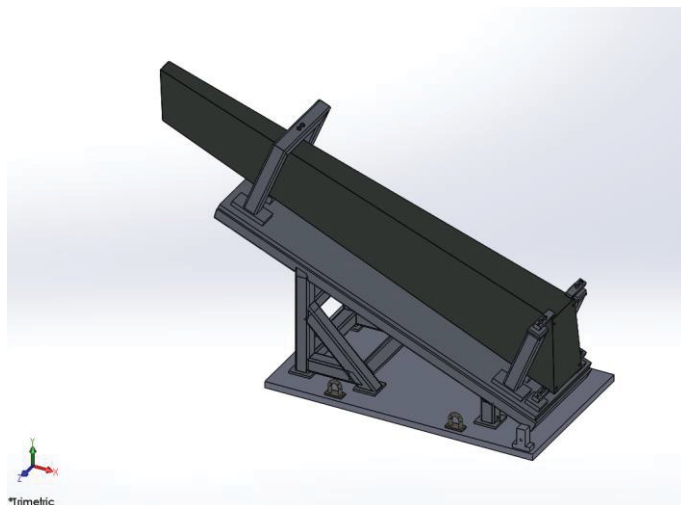


Figure 5.8. Final Assembly Trimetric View

6 Finite Element Analysis

6.1 Structural Analysis of Tail Wing

- The Final Design of the Tail wing of an Apache that is subjected to Milling process is provided by the industry. The CAD model is imported into ABAQUS.
- As the design is defence related and is confidential, the company has denied approval for publishing any further information but approved to share the procedure and the approach for the verification of the design.

6.1.1 Force Calculations

Table 6.1. Cutting Parameters

Parameter	Value
C_v (m/min)	760
D (mm)	50
N (rpm)	4837
D_c (mm)	2.54
W_c (mm)	25
F_t	0.1
N_i	4
η_m	0.85
k_{c1} (N/mm ²)	600

The Parameters in Table 6.1 were provided by industry for force calculation.
As the 4-Flute cutter is used,

$$N_i = 4$$

From equation (4.1)

$$F_r = 1934.8 \text{ mm/min}$$

Mean chip thickness,

$$\text{MCT} = F_t * \sqrt{\frac{W_c}{D}} = 0.0707$$

Specific Cutting force,

$$F_s = \frac{(1-0.01)*60*k_{c1}}{MCT} = 4.2002 * 10^5 \text{ N/mm}^2$$

From equation (4.2) and (4.3) Power required can be obtained

$$P = 1.2142 \text{ kW}$$

Cutting force into the Workpiece, i.e. Tail wing using Equation (4.4),

$$p_z = 0.5334 \text{ kN}$$

To verify the cutting forces the given data was fed into the commercial Application of Sandvik Milling Calculator.

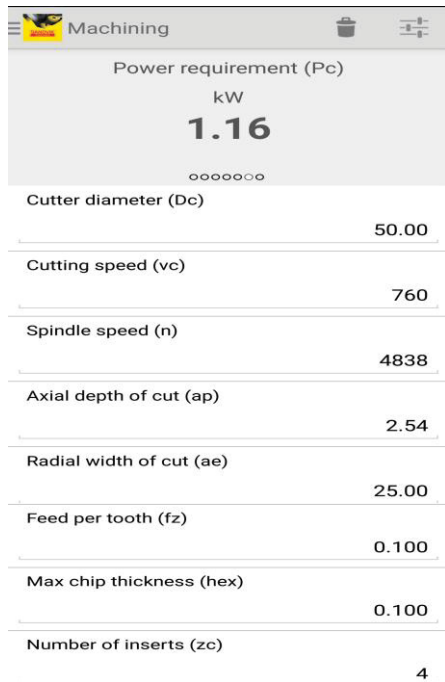


Figure 6.1. Cutting Force Calculation by Application

From Figure 6.1 the power required,

$$P_c = 1.16 \text{ kW}$$

Cutting Force is calculated from P_c ,

$$p_{zc} = 0.5396 \text{ kN}$$

Table 6.2. Comparison Between analytical and Application values

Parameters	Analytical	Application	Deviation
Power Required	1.2142 kW	1.16 kW	4.3%
Cutting Force	533.4 N	539.6 N	1.2%

From Table 6.2 it can be validated that the analytical calculations are equal to that of the calculations used by the industry.

Therefore, analysis the cutting force, p_z obtained is the force exerted on the tail wing by the milling flute.

6.1.2 Simplifications

- Due to the design complexity of the fixture and Tail Wing Assembly partitions are created in the place of fixtures on the Tail wing and are constrained at those partitions.
- The force, p_z is applied on the location at which the flute contacts the Tail Wing.

6.1.3 Analysis

- A static structural analysis is performed on the Tail wing, the Von-misses stress distribution near the mounting slots is studied and found to be low when compared to that of the Ultimate tensile strength of the material.
- The factor of safety is determined by using the formula $FS = \frac{UTS}{\sigma_{max}}$

6.1.4 Conclusion

- The factor of safety is greater than 2.1 suggests that milling operation can be performed to remove the additional material from the Tail Wing.

6.2 Structural Analysis of Base Plate

- The Base plate in the Figure 5.5 is designed in SOLIDWORKS as per the design parameters provided and is imported to ABAQUS for analysis and design check.
- Purpose: The Base plate consists of 4 d-rings to which crane hooks are attached to transport it to manufacturing area.
- Analysis Purpose: The main purpose of the analysis is to check the design strength of the base plate when the base plate is lifted off the ground.

6.2.1 Force calculations

- To lift the entire assembly equal amount of force must be applied in the opposite direction according to Newton's law.

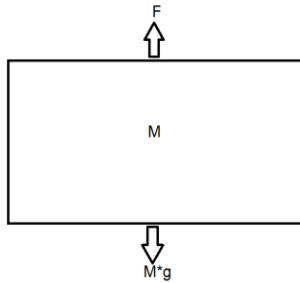


Figure 6.2. Force Diagram

- From, Figure 6.2 to lift the mass of the assembly

$$F \geq M * g \quad (6.1)$$

- M is the mass of the entire assembly, i.e., combined weight of the Top plate, Truss structure and Base plate.

Table 6.3. Mass details

Component	Mass (Kg)
Top Plate	94.35
Truss Structure	76.78
Base Plate	150.317

- The mass of the components in the Table 6.3 are provided by the industry.
- Therefore, the entire mass of the entire assembly is 321.447 Kg.
- From equation (6.1),

$$F \geq 3153.395 \text{ N}$$

- Force applied, F must be greater than 3153.395 N is approximated to 3200 N.

6.2.2 Simplifications

- The truss structure on the base plate are substituted as constraints on the base plate to decrease the computational time. As shown in the Figure 6.4.
- The weight of truss structure and the baseplate which are in contact are uniformly distributed hence the load on each d-ring could be approximated to same magnitude.
- Screw-nut assemblies are replaced by contact sets. Reference geometries which are light in weight compared to the structure on the plate are neglected.
- The threading of the screw will constraint the rotation of the D-ring as well as it gives a scope for displacement transfer by constraining the movement of the D-ring, which means a surface to surface contact would be more appropriate to replace the Screw-nut contact.
- Therefore, tying both the geometries to one another is better approximation to screw-nut contact as shown in the Figure 6.3.

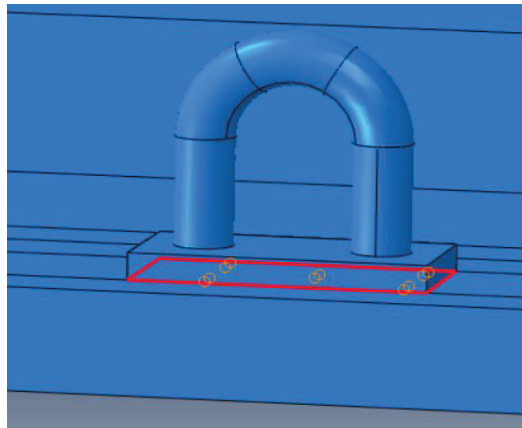


Figure 6.3. Contact Set

6.2.3 Analysis

- The model is imported to ABAQUS, appropriate partitions are made on the base plate and on the Stainless-Steel D-rings for the boundary conditions and loads respectively.
- Material properties such as Density ρ , Young's modulus ε , and poisons ratio ϑ , of Aluminium 5052 H32 and assigned to the baseplate.
- Similarly, Material properties of Stainless Steel are entered and assigned to the D-rings. It is also noted that the D-rings are used for heavy duty liftings and their strength comes from material properties.
- The D-rings and the Baseplate are tied to each other by in the contact properties.

Table 6.4. Material Properties

Properties	Stainless Steel [7]	Aluminium5052-H32 [8]
Density	8 g/cc	2.68 g/cc
Young's modulus	200 Gpa	70.3 Gpa
Poison's ratio	0.29	0.33
σ_{Yield}	205 Mpa	195 Mpa

- Four D-rings are present to lift the base plate therefore load on each D-ring.

$$\frac{3200}{4} = 800 \text{ N}$$

- The load is applied in terms of pressure along the contact area on the D-rings and the lifting equipment.
- Area of Contact on D-rings is length of the arc times the thickness of the D-ring,

$$A_d = L_A * T_d$$

- Length of the arc of contact of the chains from the crane with D-ring,

$$L_A = 2 * \pi * r * \frac{\theta}{360} \quad (6.2)$$

$$L_A * T_d = 2 * \pi * 22.39 * \frac{90}{360} * 20 \text{ mm}^2$$

- Load in terms of pressure,

$$P_d = \frac{800 \text{ N}}{A_d}$$

$$P_d = 1.14 * 10^6 \text{ Pa}$$

- Partitions are made on each D-ring with the acquired area of contact, A_d and the pressure, P_d is applied on the partitions in positive y direction.

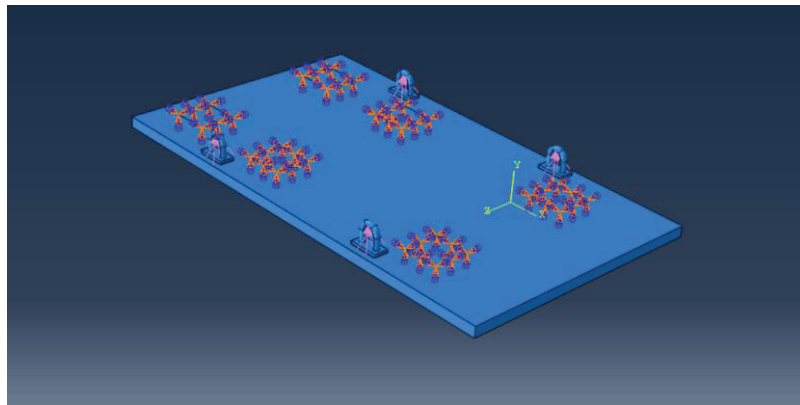


Figure 6.4. Location of boundary conditions and loading

- Figure 6.4 shows the positions of boundary conditions and the location of load applications.
- A tetrahedron free mesh is used for meshing the geometry, quadratic shape function is selected for more accuracy of the results [9].
- The element size is chosen by making use of convergence plot from Figure 6.5 of the stresses on the plate.
- The results are presented in Appendix.

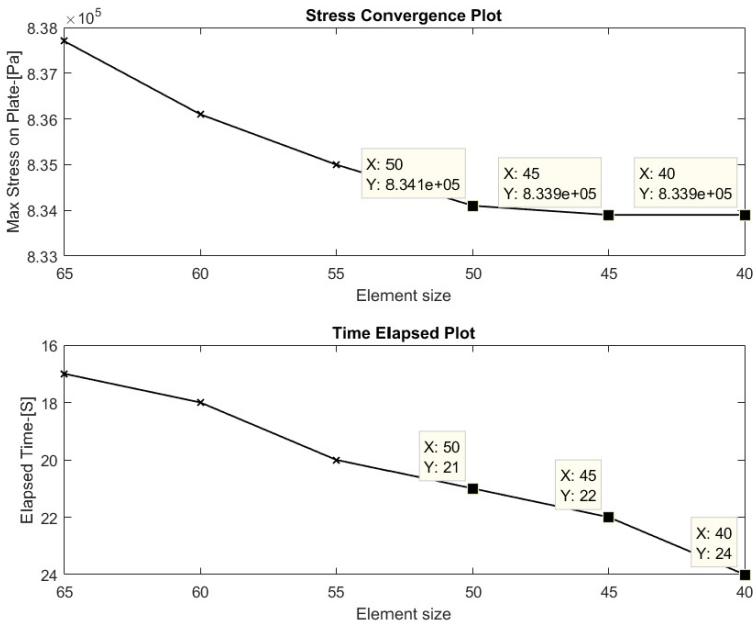


Figure 6.5. Convergence Plot

- From Figure 6.5 it is observed that the maximum stress value on the base plate is converged in the decreasing order, also the time elapsed is presented in the reverse sense to make a better comparison and approach towards the selection of element size.
- The selection of element size can be performed by visual interpretation of the graphs minimal distance of the data tips from each plot at their respective average element size; therefore, element sizes 50, 45, 40 are selected in the primary assessment.
- In the secondary assessment as the stress value is getting converged at element size 45, element size 50 is ruled out. The third visual assessment, i.e. by comparing the distance between the data tips, element size 45 is selected for presentation as well as for future analysis requirements.

6.2.4 Result

- The job is submitted for analysis. Figure 6.6 shows the stress distribution on the baseplate and Figure 6.7 shows the magnitude of deformation of the baseplate in Y- direction.

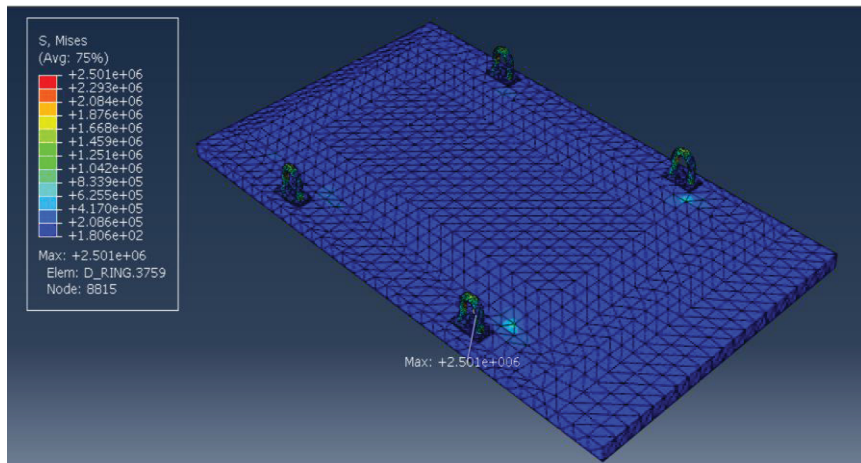


Figure 6.6. Von-Misses Stress Distribution on Baseplate

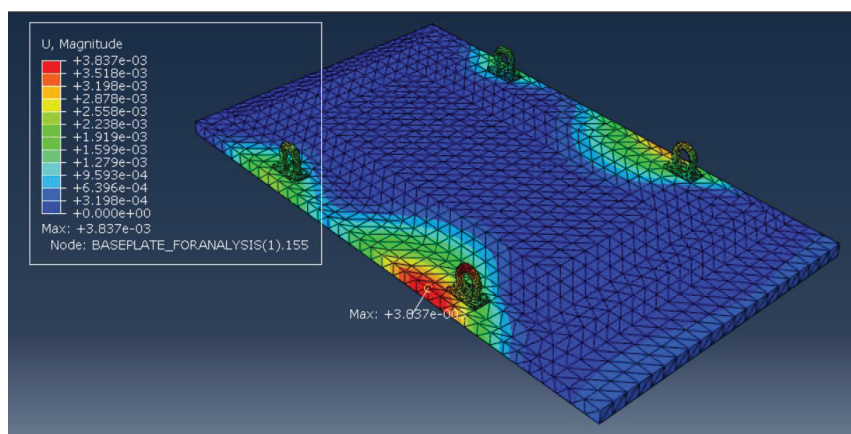


Figure 6.7. Deformation of Baseplate

6.2.5 Conclusion

- From Figure 6.8 it is observed that the stress distribution is directed towards the point of application of load.

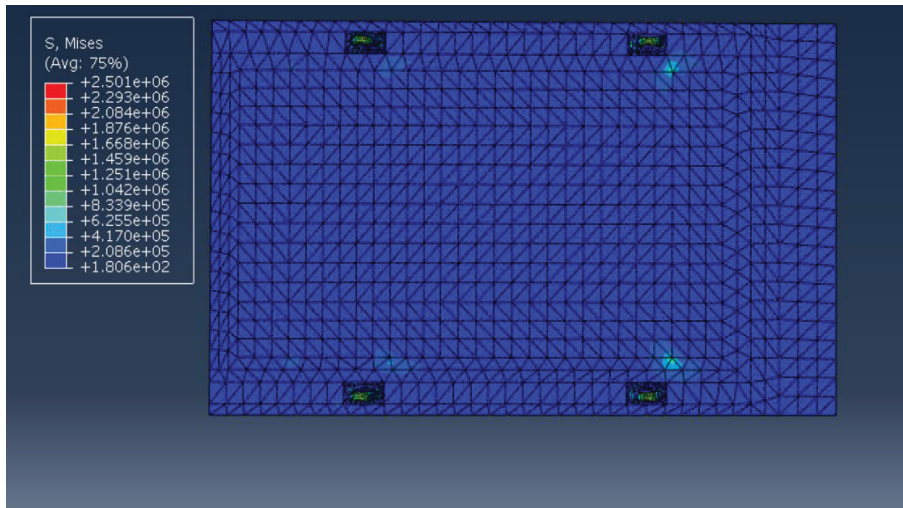


Figure 6.8. Von-Misses Stress Distribution Baseplate Top view

- The baseplate is not symmetrical with respect to X-axis, this can be clearly observed from Figure 5.5 and Figure 5.6 also from Figure 6.4 the constraints on the baseplate are unsymmetrical, which implies that the D-ring which is close to the edge of the baseplate and is far from constraints is subjected to more displacement than that of other D-rings, despite of the fact that equal amount of load is applied on all the D-rings.
- The maximum stress is observed on the D-rings, which is because they are constrained to the base plate close to the point of application of load. A detailed view of the location of maximum stress is presented in Figure 6.9.
- A detailed view of maximum stress on D-ring and baseplate are presented in Appendix

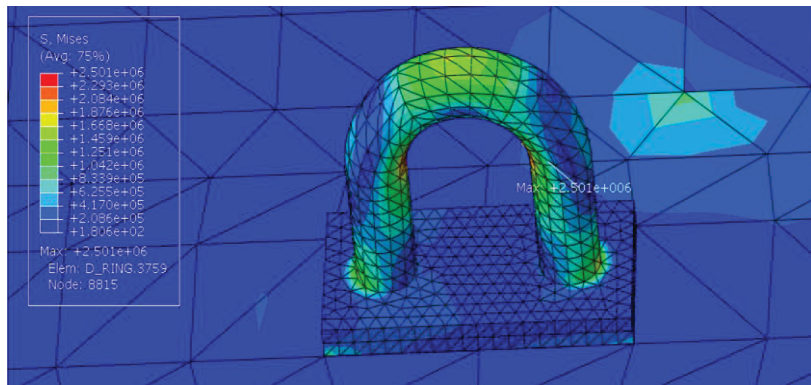


Figure 6.9. Zoomed view of maximum stress on D-ring

Table 6.5. Maximum Stress V/s Yield Strength

Component	Maximum Stress	Yield Strength
D-ring	2.501 Mpa	205 Mpa
Base Plate	0.8339 Mpa	195 Mpa

- From Table 6.5 the maximum stress on both the base plate and the D-ring are under the allowable value of yielding of the materials and hence the design strength is acceptable for the working conditions.

7 Validation

The work presented in this chapter is carried out at the industry which provides the actual analysis and parameters carried out at the industry. On request, the industry has provided access to present this 2D design and analysis is carried out for the validation purpose.

For the validation of the base plate design a shell element is considered and assigned to the base plate in Abaqus CAE. The reason to consider a 2D shell element is that whatever may be the environment the type of force acting on the base plate will be the same and should have a similar bending and stress distribution, if that was achieved then it could be said that the design created is suitable for its functionality. The shell arrangement is applied because with solid element in Finite Element Method for bending problem the disadvantage is Locking. Locking is a phenomenon which occurs during bending, in the solid element the bending behaviour is much stiffer when compared with the analytical solution. Locking can occur for several reasons in some elements. Locking also depends on the shape of the elements however it is seen that locking happens only when an element cannot interpolate a field property nodal values and the element shape functions. Table 7.1 depicts the mass details of the actual design.

Table 7.1. Actual Mass of the Components

Component	Mass in Kilograms
Truss Structure	96.32
Top Plate	108.65
Base Plate	145.43

7.1 Force Calculation

The base plate of the Jig and the Fixture assembly consists of D-rings that are used for lifting the Jig and the Fixture for moving it from one place to another. To lift any object from its equilibrium position, one should exert a

force higher in magnitude in the opposite direction to the force being exerted by the object.

- Table 7.1 gives the information about the total weight of the system which is 350.4 Kg.
- The force acting on the ground by the system Jig and Fixture is 3437.42N. For being able to lift the Jig and fixture assembly a force that is greater to 3437.42N is to be applied in the opposite direction.

$$F_2 \geq 3437.42 \text{ N}$$

- Hence the force being applied to lift the Jig and Fixture assembly is approximated to be 3450 N

7.2 Simplifications

- The Jig and Fixture is lifted with the help of Four D-Rings hence the force subjected on each D-Ring is assumed to be equal therefore, the force on each D-Ring

$$F_{2D} = \frac{3450}{4} = 862.5 \text{ N}$$

- The Truss arrangement on the base plate are taken as constraints.

7.3 Analysis

- The actual design from the industry is converted to a 2D design for simplification of the analysis.
- The base plate is designed as a 2D shell element in ABAQUS.
- The d-rings are substituted as partitions on the base plate. As the lifting equipment makes contact with the partitions, 20X40 mm

partitions are made on the d-rings. As well as the positions at which the truss contacts the base plate.

- The pressure that is required for lifting of the Jig and Fixture is applied on the 20X40 mm partition mentioned earlier.

$$P_{2D} = \frac{F_{2D}}{A_{2D}}$$

$$P_{2D} = 1.07 * 10^6 \text{ Pa}$$

- A shell element type mesh is selected for a better accuracy of the result.

7.4 Result

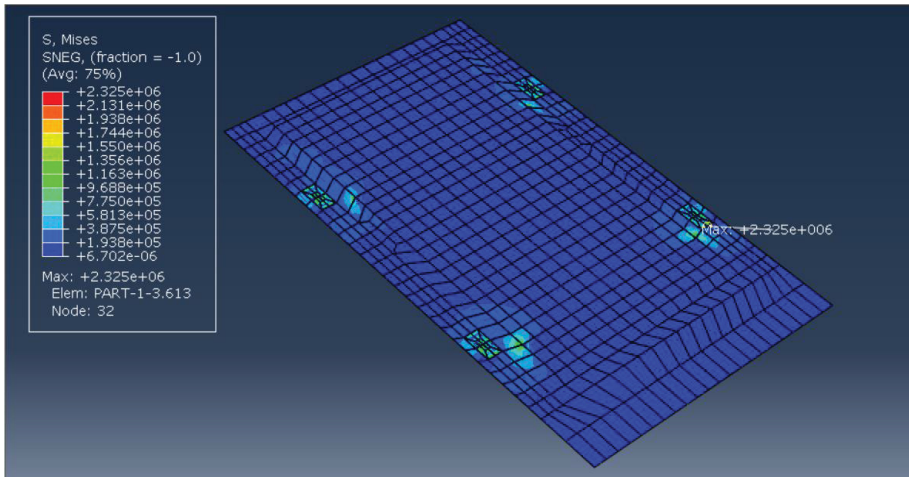


Figure 7.1. Von-Misses Stress distribution on shell plate

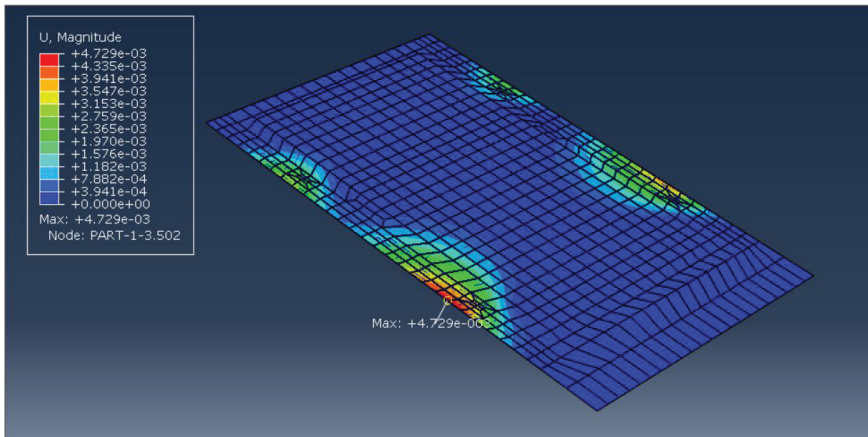


Figure 7.2. Deformation of the 2D baseplate

7.5 Conclusion

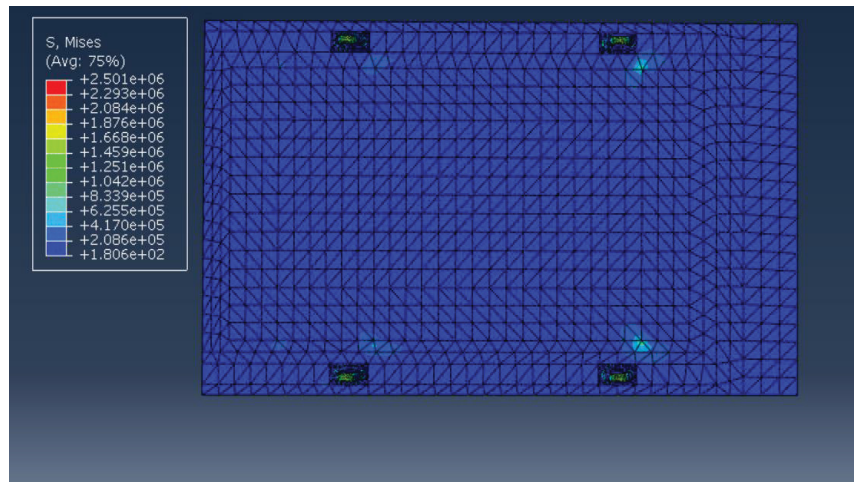


Figure 7.3. Von-Misses Stress distribution 3D analysis

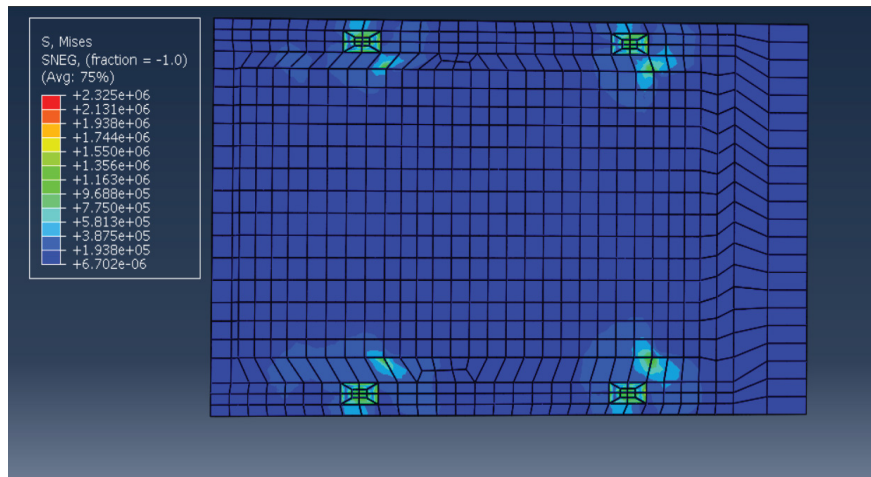


Figure 7.4. Von-Misses Stress distribution 2D plate

Table 7.2. Maximum Stresses

Analysis	3-Dimensional	2-Dimensional	Deviation (%)
On D-ring	2.501 Mpa	2.325 Mpa	7.2
On Plate	0.8339 Mpa	0.775 Mpa	7.6

- From Figure 6.7 and Figure 7.2 the maximum deformations are 3.422 mm and 4.729 mm respectively, showing a deviation of 27% this deviation is because of the fact that solid elements show more stiffness when compared with that of shell elements hence shell elements show more deflection.
- From Table 7.2 the maximum stresses on the plates and the D-rings are equal suggesting that the design and the analysis presented in the Section 6.2 is equal to the design and analysis performed at the industry.

8 Design Iterations

The base plate with three different thickness values are readily available with the suppliers to the company. Therefore, performing FE analysis on them would provide the industry with some design guidelines. The interesting aspect is that as the thickness of the base plate decreases the self-load (the load on the base plate) decreases. Hence to check the stress distribution on the baseplate, three iterations are carried out. All the three iterations are carried out by following the similar steps that are carried while performing analysis on the baseplate with thickness 38mm.

8.1 Force Calculations

Table 8.1. Thickness V/s Assembly Mass

Thickness of base plate	Mass of base plate(Kg)	Assembly Mass (Kg)
35	138.23	309
30	118.9	290
25	99.6	270.73

- The force on Design iteration-1 (35mm plate thickness),
$$F_3 \geq 3031.29 \text{ N}$$
- The force on Design iteration-2 (30mm plate thickness),
$$F_4 \geq 2844.9 \text{ N}$$
- The force on Design iteration-3 (25mm plate thickness),
$$F_5 \geq 2655.86 \text{ N}$$

8.2 Analysis

- The CAD models are imported into ABAQUS, appropriate partitions are made on d-rings and on the baseplate for application of loads and boundary conditions.
- Material properties such as Density ρ , Young's modulus ϵ , and poisons ratio ϑ , of Aluminium 5052 H32 and Stainless steel are entered in the properties section.
- The D-rings and the Baseplate are tied to each other by in the contact properties.

8.2.1 Design Iteration - 1 ($T = 35 \text{ mm}$)

- The total force on the baseplate, F_3 is approximated to 3090 N.
- The load on each d-ring,

$$\frac{3090}{4} = 772.5 \text{ N}$$

- As the contact area of the equipment with the d-ring remains the same hence,

$$P_{3d} = 1.1 * 10^6 \text{ Pa}$$

- The pressure, P_{3d} is applied on the partitions of the d-rings.

8.2.2 Design Iteration - 2 ($T = 30 \text{ mm}$)

- The total force on the baseplate, F_4 is approximated to 2900 N.
- The load on each d-ring,

$$\frac{2900}{4} = 725 \text{ N}$$

- As the contact area of the equipment with the d-ring remains the same hence,

$$P_{4d} = 1.03 * 10^6 \text{ Pa}$$

- The pressure, P_{4d} is applied on the partitions of the d-rings.

8.2.3 Design Iteration - 3 ($T = 25 \text{ mm}$)

- The total force on the baseplate, F_4 is approximated to 2700 N.
- The load on each d-ring,

$$\frac{2700}{4} = 725 \text{ N}$$

- As the contact area of the equipment with the d-ring remains the same hence,

$$P_{5d} = 0.96 * 10^6 \text{ Pa}$$

- The pressure, P_{5d} is applied on the partitions of the d-rings.

8.3 Results

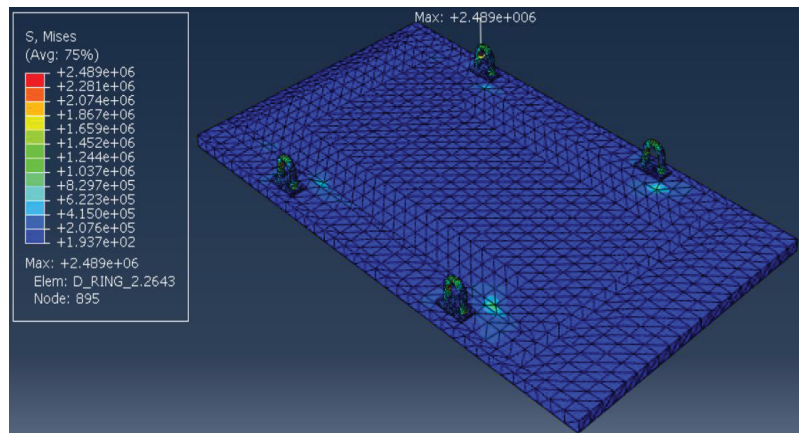


Figure 8.1. Von-Misses Stress distribution for 35mm thickness plate

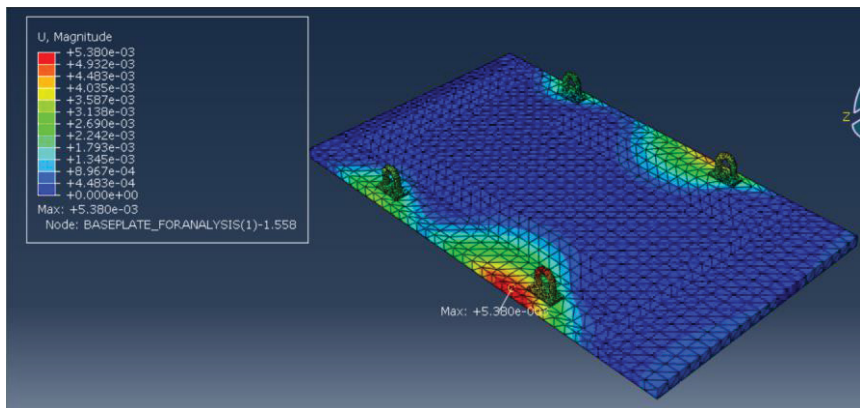


Figure 8.2. Deformation of 35mm plate

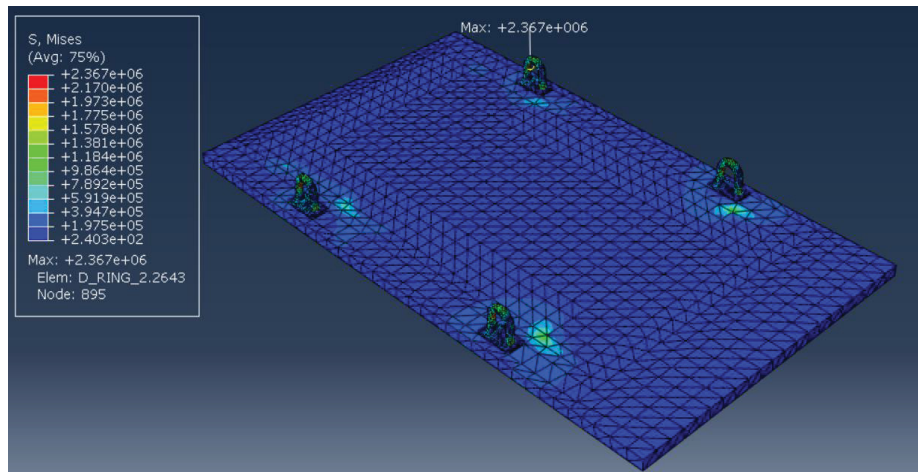


Figure 8.3. Von-Misses Stress distribution on 30mm thickness plate

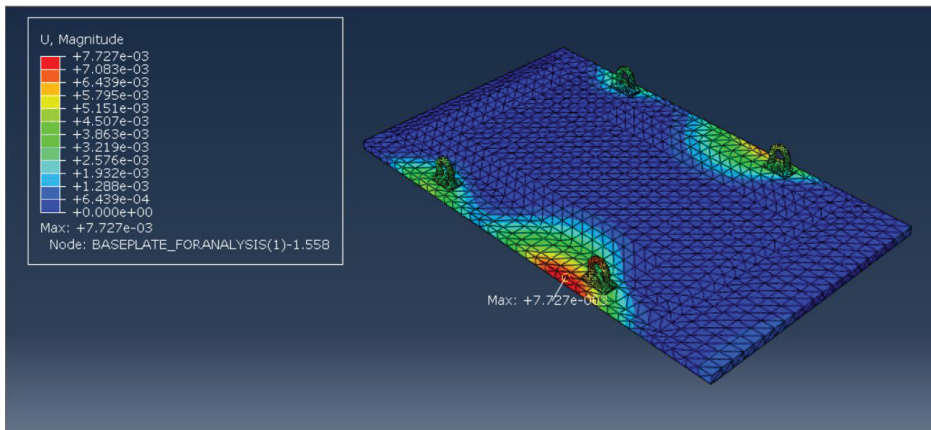


Figure 8.4. Deformation of 30mm plate

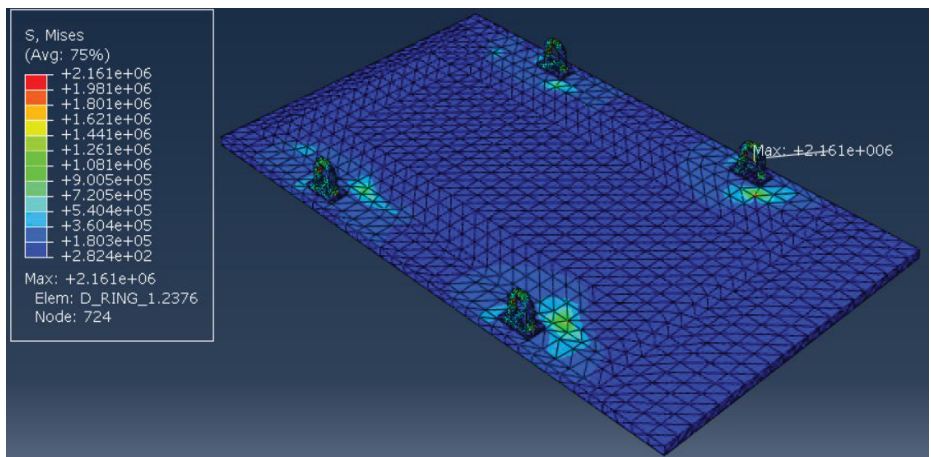


Figure 8.5. Von-Misses Stress distribution on 25mm plate

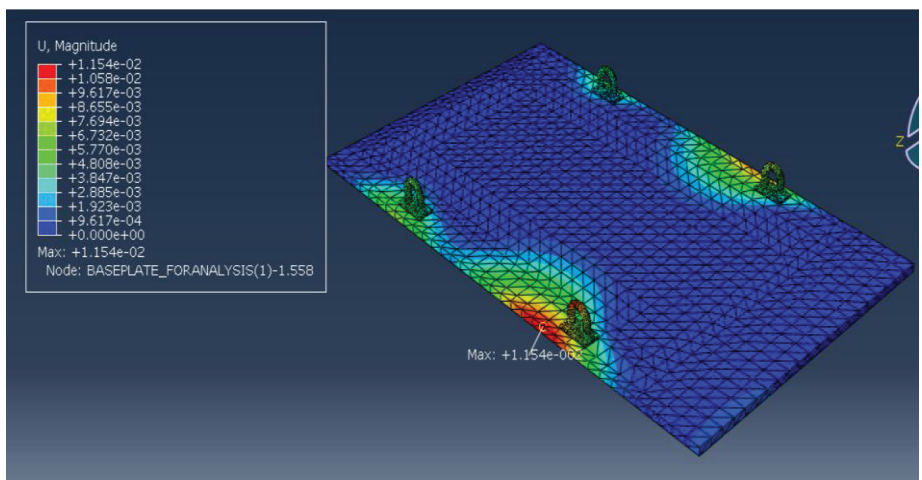


Figure 8.6. Deformation of 25mm plate

Table 8.2. Maximum stress values

Thickness of base plate	On D-ring	On Baseplate
35	$2.489 * 10^6$ Pa	$0.879 * 10^6$ Pa
30	$2.367 * 10^6$ Pa	$0.986 * 10^6$ Pa
25	$2.161 * 10^6$ Pa	$1.091 * 10^6$ Pa

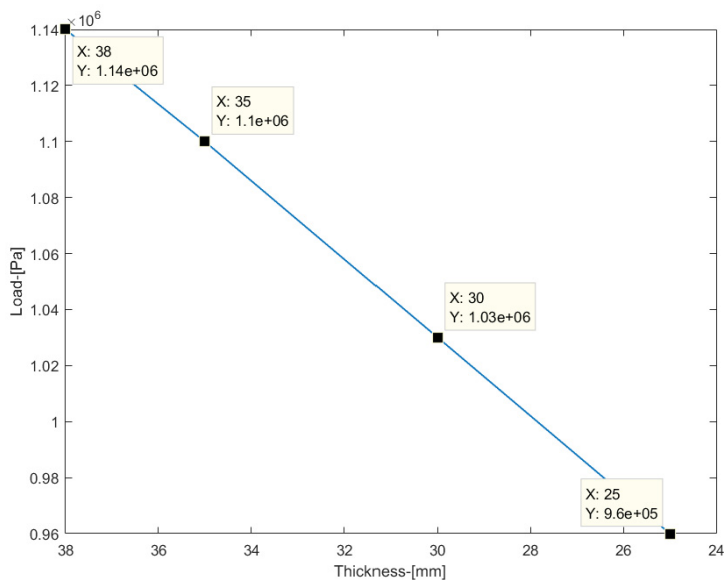


Figure 8.7. Variation of load on each D-ring with thickness

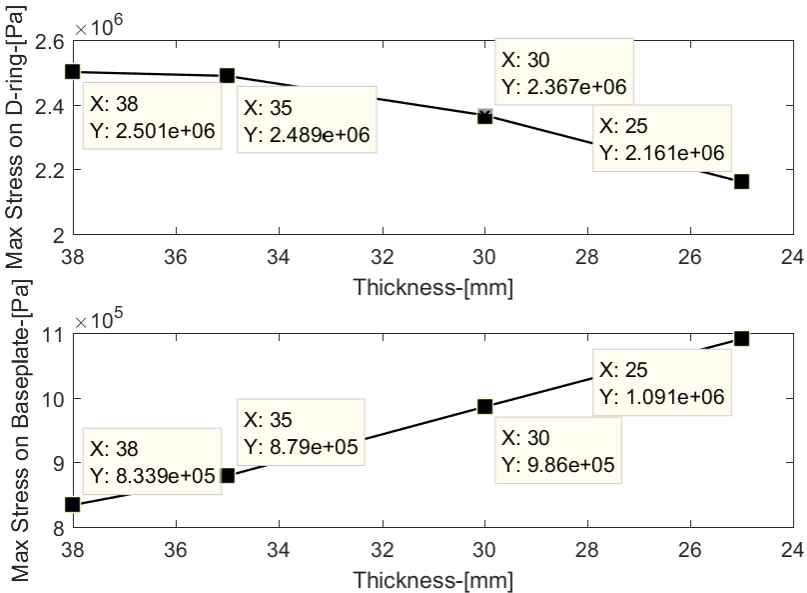


Figure 8.8. Variation of maximum stress with thickness

8.4 Discussions and Conclusions

1. Figure 8.7 and Figure 8.8 shows variation of loads and maximum stresses with the decrease of thickness of the baseplate respectively.
2. From Figure 8.8 it can be observed that the maximum stress on the D-rings is decreasing with the thickness of baseplate whereas maximum stress on the baseplate is increasing. This is because the load applied in each iteration is decreasing as the thickness of the baseplate is decreasing whereas the thickness of the D-ring remains constant throughout all the iterations.
3. The D-rings are standard components that are readily available, designed to withstand heavy loads and so are made of Stainless Steel. They are not considered as the same material that of baseplate (Aluminium) at the time of analysis to match the real scenario.
4. As the plate with 25mm thickness is the least thickness readily available, the maximum stress on the D-ring and the base plate are compared with yield strength.

Table 8.3. Maximum Stress on 25mm baseplate

Component	Maximum Stress	Yield Strength
D-ring	2.161 Mpa	205 Mpa
Base Plate	1.091 Mpa	195 Mpa

5. From Table 8.3 it can be concluded that a 25mm baseplate can be used instead of 38 mm thickness base plate.
6. The research questions from the Section 2.4 are outlined as follows:
 - a. Can the design sustain the milling operation with the given cutting parameters?
 - The cutting forces from the milling tool are calculated by using concept of MCD, showing a good correlation with the forces from Sandvik Milling Calculator. The Factor of safety suggests that the induced Von-misses stress on the tail wing are well with the limits of tensile strength. Thereby suggesting the machining process can be carried out with given cutting parameters. The research contributed literature for future references on the estimation of cutting forces, types of milling operations, purpose of jig and fixture, evaluating the design strength while performing milling operation on vital components to the industry.
 - b. Can the baseplate sustain the weight of the entire structure when lifted during the transportation of the jig-fixture assembly without yielding?
 - The design strength of the baseplate is checked for yielding when the structure is lifted-off from the ground for transportation, to avoid the instability of the baseplate. Therefore, the weight of the entire structure is given as force (required to lift) to the D-rings to check the stress distribution. The stress distribution on the baseplate and on the D-rings indicated that the maximum stress is well within the yielding limits. Also, the results obtained from the 2-D analysis that was carried at the industry showed correlation with 3-D

analysis. The maximum stress from the Table 6.5 indicated the design strength of both baseplate and D-rings will not yield for working loads. The results and analysis procedure has given a good idea on checking the design strength of large plates that support heavy loads. Also, literature on the factors or the forces acting during lift-off condition.

- c. What is the best possible thickness of the baseplate for the working loads that is readily available?
 - Once the design strength of the 38mm baseplate is checked for yielding, the material suppliers are contacted and data about available baseplate raw materials with varying thicknesses i.e., 35mm, 30mm, 25mm is collected. Therefore, three more iterations are carried out to check the design strength of each baseplate. On comparing the Von-misses stress obtained from each iteration, it is concluded that the baseplate with thickness 25mm is the lightest, utilises less material out of all the other plates and is the best possible design (thickness) available for the working conditions.

9 Future work

- The top plate and the truss assembly are already designed and forwarded to the manufacturing shop by the time the thesis commenced. Therefore, the top plate and the truss assembly were not studied efforts could be put in studying the design and optimization of top plate and truss assembly for the future endeavours.
- Evaluation of the strength of the design is performed for the existing model and the design iterations performed as well are the available designs with supplier. There are other ways to provide design guidelines to the industry as well by performing a structural and topology optimization of the baseplate.
- The lifetime in cycles of the baseplate can be estimated by fatigue calculations.

10 References

- [1] M. C. Shaw, *Metal cutting principles*, 2nd ed. New York: Oxford University Press, 2005.
- [2] B. M. Swami, K. S. R. Kumar, and C. H. Ramakrishna, “Design And Structural Analysis Of Cnc Vertical Milling Machine Bed,” *Int. J. Adv. Eng. Technol.*, vol. 3, no. 4, pp. 97–100, 2012.
- [3] S. K. H. Choudhary and S. K. Bose, *Elements of Workshop Technology*, 4th ed., vol. II : Machine Tools. Bombay: Media Promoters & Publishers PVT.LTD.
- [4] S. Patel, S. Vasoya, and A. Joshi, “DESIGN AND MANUFACTURING OF JIGS FOR DRILLING MACHINE,” 2017.
- [5] “Metal_Cutting_Principles_2nd_Edition_-_By_Milton_C._Shaw.pdf.” .
- [6] S. S. Pachbhai and L. P. Raut, “A review on design of fixtures,” *Int. J. Eng. Res. Gen. Sci.*, vol. 2, no. 2, pp. 2091–2730, 2014.
- [7] ASM International, Ed., *ASM handbook*, 10th editon. Materials Park, Ohio: ASM International, 1990.
- [8] A. S. M. International, A. I. H. Committee, and A. I. A. P. D. Committee, *Metals Handbook: Properties and selection*, vol. 2. Asm International, 1990.
- [9] G. Broman, *Computational Engineering*. Department of Mechanical Engineering, Blekinge Institute of Technology, Karlskrona, Sweden, 2003.

11 Appendix

11.1 MATLAB CODE

```
%% Calculation of Cutting Forces
clc;
clear all;
% Given data
C_v = 760; %m/min % Cutting Speed
D = 50;%mm % Diameter
N = 4837;%r.p.m % spindle Speed
D_c= 2.54; % mm %depth of cut
W_c =25 ;%mm %width of cut
F_t=0.1 ;%Feed/tooth
N_i =4 ;%number of inserts
Neta=0.85; %Efficiency
% Calculations
F_r = N*N_i*F_t;%mm/min %feed rate
K_C1 = 600; % Specific cutting force for Aluminium(si<12%) for 1mm2
M_CT = F_t*sqrt(W_c/D);% mean chip thickness
F_s=(1-0.01)*60*K_C1/M_CT;%n/mm2 %specific Cutting Force
P_z=F_s*W_c*D_c/(6*10^7) ; % Cutting force % Converting mm to m
%Also F_s*W_c*D_c = M.R.R
P = P_z*F_r/(Neta);% power required in Kw
```

11.2 Partitions

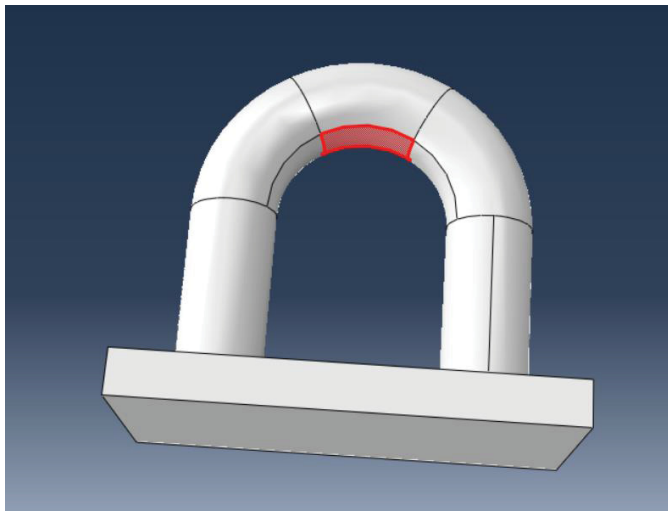


Figure 11.1. Partition on D-rings

11.3 Results from FE – analysis

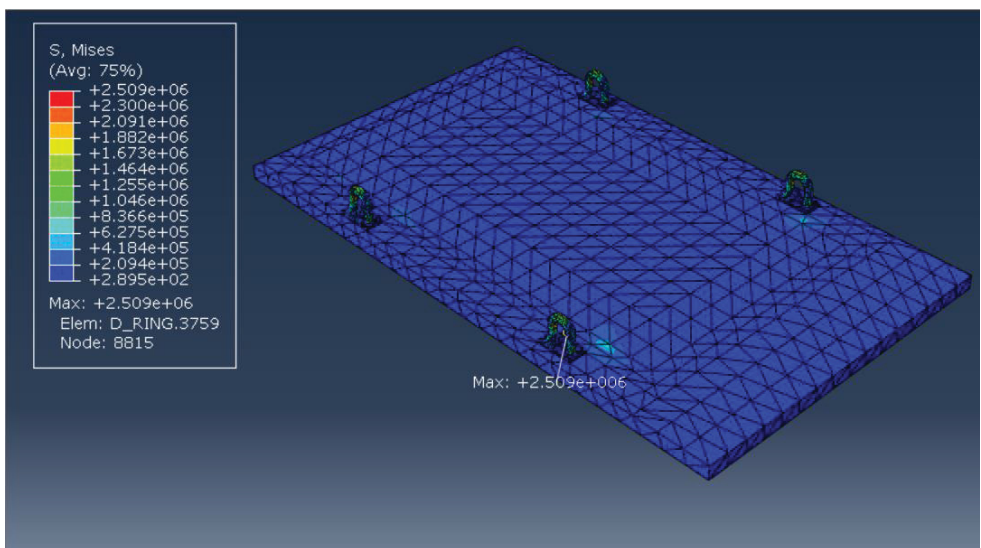


Figure 11.2. Stress distribution with average element size 65

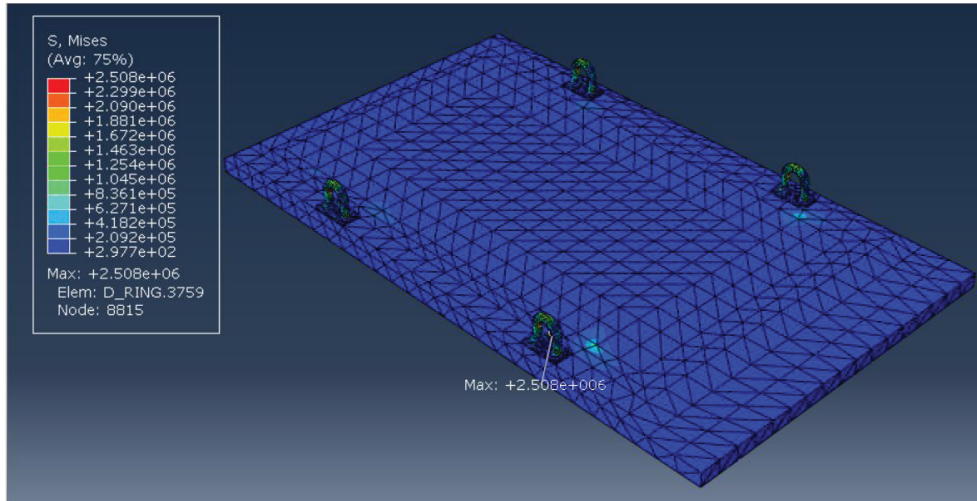


Figure 11.3. Stress distribution with average element size 60

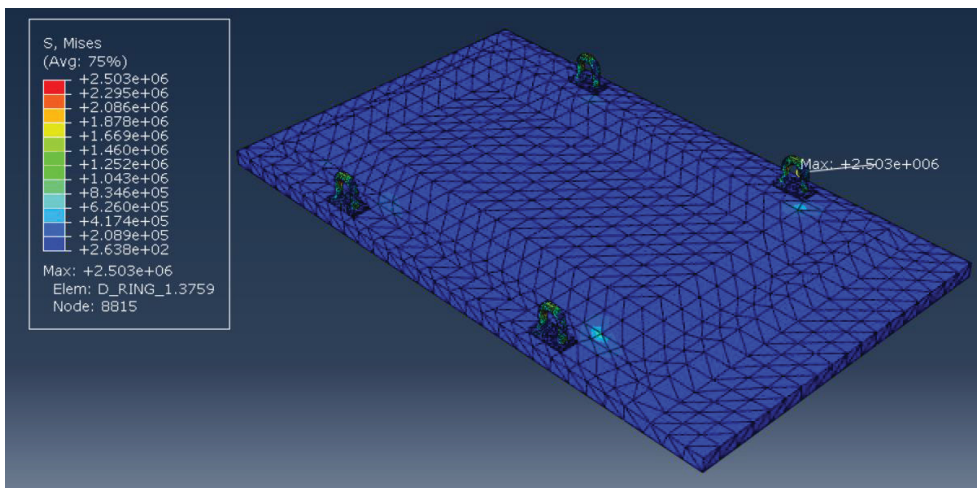


Figure 11.4. Stress distribution with average element size 55

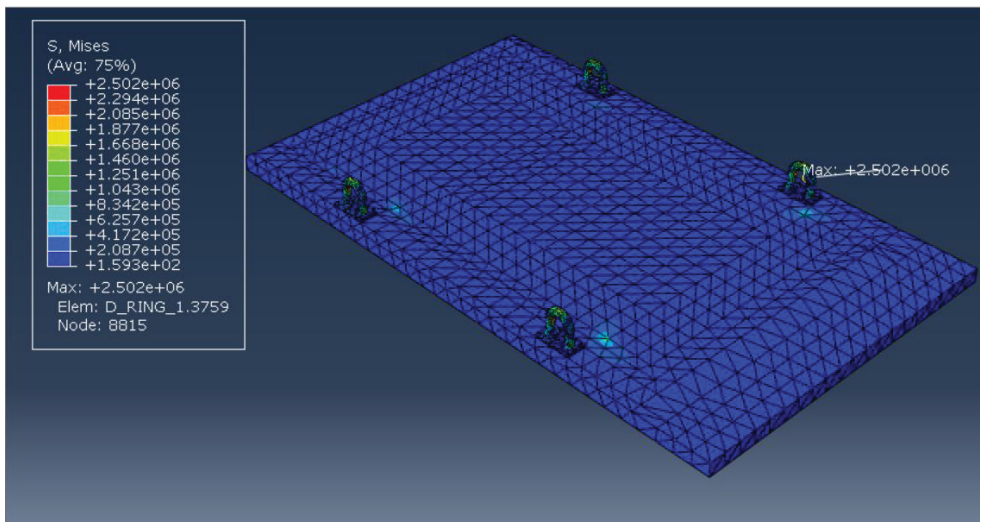


Figure 11.5. Stress distribution with average element size 50

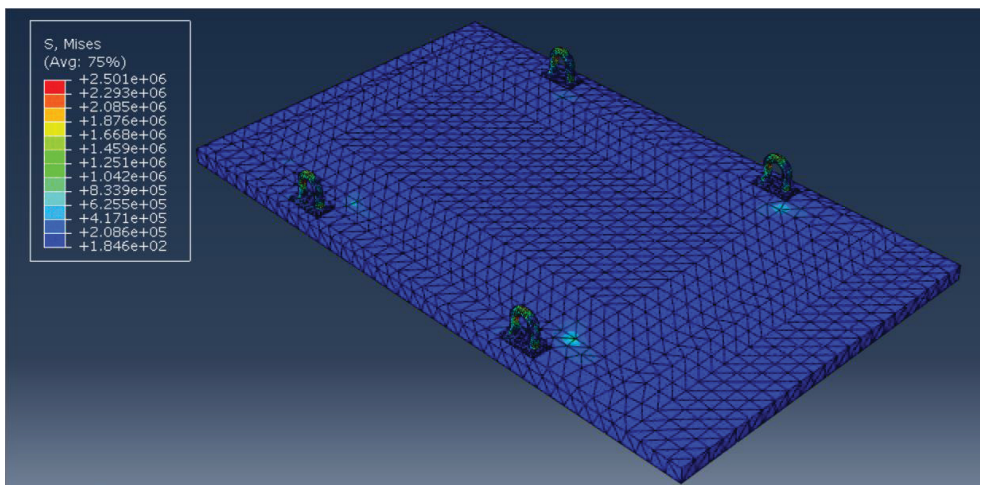


Figure 11.6. Stress distribution with average element size 40

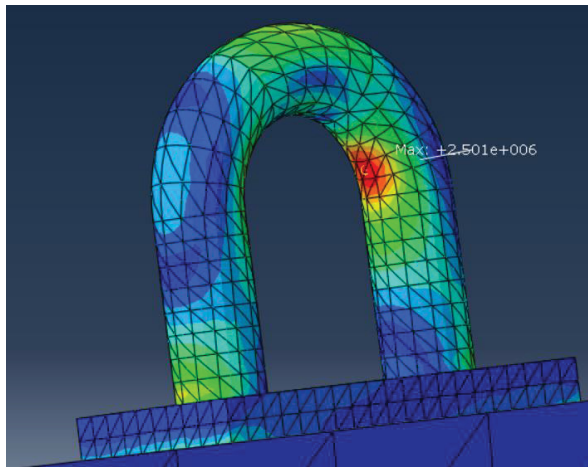


Figure 11.7. Detailed View of stress distribution on D-ring

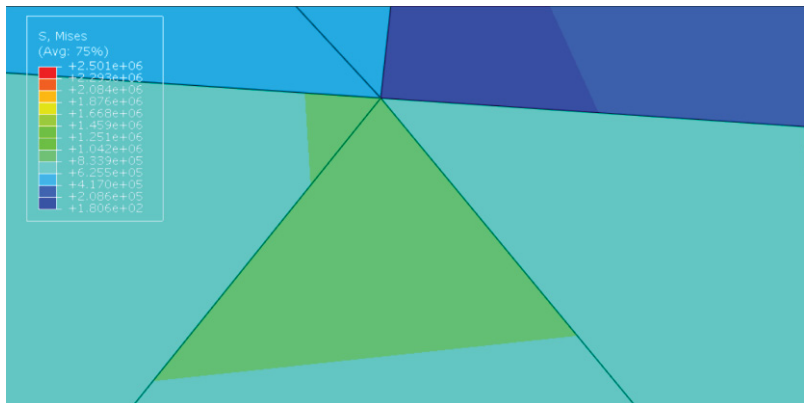


Figure 11.8. Detailed view of Max Stress on Baseplate



Department of Mechanical Engineering
Blekinge Institute of Technology
SE-371 79 Karlskrona, SWEDEN

Telephone: +46 455-38 50 00
E-mail: info@bth.se